Influence of Iodine Merz-Singh-Kollman Radius on the Calculated Charges and Hydration Free Energies of Iodinated Molecules

Andreia Fortuna,[a,b,c] Pedro M. S. Suzano[a,b], Miguel Machuqueiro[a,b], Paulo J. Costa[a,b*]

[a]*BioISI – Instituto de Biossistemas e Ciências Integrativas, Faculdade de Ciências, Universidade de Lisboa, 1749-016, Lisboa, Portugal*
[b]*Departamento de Química e Bioquímica, Faculdade de Ciências, Universidade de Lisboa, Lisbon, Portugal*
[c]*Research Institute for Medicines (iMed.ULisboa), Faculty of Pharmacy, University of Lisbon, Av. Professor Gama Pinto, 1649-003 Lisbon, Portugal*

Empirical force field methods typically rely on point charges to describe the electrostatic interactions, which is problematic when anisotropy needs to be considered, as in the case of the electrostatic potential of covalently-bound halogens that possess a positive site, termed σ–hole, surrounded by a large negative belt. To address this, an off-center point charge (EP) is usually placed at a given distance from the halogen to emulate the σ–hole and commonly-used implementations are based on the Restrained Electrostatic Potential (RESP) procedure to fit atomic charges, being one of the most used charge models. In this context, no specific Merz-Singh-Kollman (MK) radius for iodine is available in the literature, which is an essential parameter in the RESP fitting procedure. In this work, we explored the impact of the iodine MK radius on the obtained RESP charges for a set of 12 iodinated molecules. We verified that the relative root mean square (RRMS) values obtained with and without an EP kept decreasing with increasing radii for most compounds, thus impairing optimization using such a procedure. Nevertheless, the use of an iodine MK radius lower than 2 Å is not advisable since the RRMS kept decreasing considerably until this value was reached. Moreover, the performance of three iodine MK radii was studied with the estimation of the free energy of hydration (ΔG_{hyd}) values using alchemical free energy calculations, which are particularly sensitive to the charges used. Despite the usage of different radii not leading to remarkable differences, our results indicate that using a value of 2.70 Å leads to lower mean absolute errors (MAE) and root mean squared error (RMSE) values when comparing the calculated with the experimental ΔG_{hyd} values.

Keywords: halogen bonds; σ–hole; RESP charges; electrostatic potential; alchemical calculations

*Email: pjcosta@ciencias.ulisboa.pt

1. Introduction

The description of electrostatic interactions in classical molecular dynamics (MD) simulations typically relies on a Coulombic pairwise potential involving atom-centered partial charges, which are critical for the accuracy and reliability of conventional force fields. However, since partial charges are not quantum mechanical observables, there is no "true" charge, and thus, various schemes for assigning atomic partial charges have been suggested in the literature. One of the most used methods, especially for the AMBER force field, is the restrained electrostatic potential (RESP)[1] charge model. This model derives atomic charges based on a fit to the electrostatic potential (ESP). The ESP, unlike partial charges, is a quantum mechanical observable. The introduction of restraints in the form of a penalty function into the fitting process prevents physically unreasonable values of the fitted charges, being responsible for its broad success.[2] Notice that not every parameter within a given model (e.g. a force field) corresponds to a physically meaningful observable. The description of the polarization of the electronic clouds, which can deeply affect the interaction between molecules, is still a challenge for non-polarizable force fields. This is particularly problematic for covalently-bound halogen atoms, that despite being considered electronegative species acting as nucleophiles, exhibit an anisotropic ESP, leading to the existence of a localized region of depleted electron density, called σ–hole[3] (Figure 1). This positive region allows halogens (X = Cl, Br, I) to interact with Lewis bases (B) establishing a directional non-covalent interaction of the R–X$\cdots$B type called halogen bond (XB).[4,5] Moreover, since X still typically possesses a large negative belt around the R–X covalent bond, it is also able to interact with electropositive species establishing hydrogen bonds (HBs). These characteristics are responsible for the interaction of halogenated molecules with biological targets such as proteins,[6–8] nucleic acids,[9] and phospholipids of the cell membrane,[10] as well as for the application of XBs in catalysis[11,12] supramolecular chemistry[5,13] and other areas of the chemical sciences.

Polarizable force fields (FFs) can eventually provide a more detailed descrip-
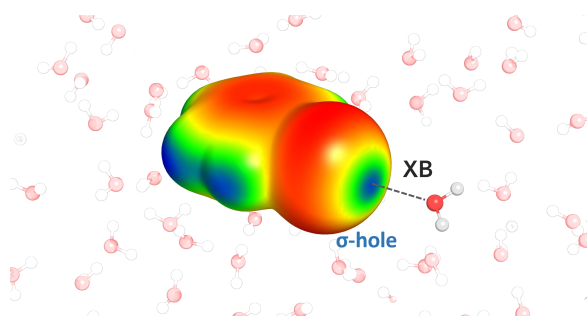
Fig. 1. Scematic representation of a halogen bond (XB). The σ–hole (blue region on the ESP) can interact with a Lewis base (e.g. a water molecule).

tion of the electrostatics, however, non-polarizable FFs are still more commonly used due to their lower computational cost. In this context, the most simple and computationally cheap strategy to emulate the σ–hole in halogen atoms is the addition of off-center point charges.[14–17] This strategy consists of the placement of a positive charge, usually called an extra point (EP), at a specific distance from the halogen along the R–X axis. Most EP implementations were developed in the context of the general amber force field (GAFF) and rely on the assignment of RESP charges. For instance, in the model proposed by Ibrahim,[14,18] the EP is placed at a distance equal to the R_{min} Lennard-Jones (LJ) parameter of the halogen and the charges of all particles, including the EP, are fitted according to the RESP procedure. During the RESP fitting procedure, also known as the Merz–Singh–Kollman (MK) scheme,[19] van der Waals radii (or MK radii) are required to build layers of grid points around the molecule. Then, atomic charges are fitted to reproduce the molecular electrostatic potential, typically obtained by QM calculations. Surprisingly, no specific MK radius for iodine is available despite RESP charges for iodinated molecules have been reported in the literature.[14,20–22] In such cases, the radius assigned to iodine is unknown. Notice that in Gaussian 09, the calculation requires that a specific radius is set in the input file whereas in GAMESS-US a value of 1.8 Å is attributed by default to elements lacking specific MK radius. Since this value is clearly too small, a value of 2.3 Å (used in Gaussian 09 for bromine) has been adopted by us in several projects.[15–17] To the best of our knowledge, only another value was reported in a recent study,[23] where the effect of the EP on the atom-centered partial charges in halogenated molecules was investigated. In this case, a radius of 2.7 Å was used to fit the atomic charges.

We recently performed the assessment of halogen off-center point-charge models using explicit solvent simulations.[24] In this study, we were surprised by the fact that introducing an EP in the RESP charge-fitting procedure for iodinated molecules yielded no advantage whatsoever over models without the EP for iodinated molecules while an improvement of the calculated hydration free energy (ΔG_{hyd}) when compared with the experimental ones, was obtained for brominated and chlorinated molecules. This fact could be, in principle, attributed to the reduced size of the iodinated dataset used (12 compounds) and their character (mostly hydrophobic and with mild to weak σ–holes). We wondered if those effects could be exacerbated by the usage of an arbitrary MK radius for iodine during the charge fitting procedure. Nonetheless, while it is true that an improvement in the calculation of ΔG_{hyd} is not evident when using an EP, especially for iodinated species, it is also true that without emulating the halogen anisotropy the formation of XBs is not possible using classical force fields,[8,25] thus impairing a proper sampling of the configurational space of the systems.[10,15] The question if EPs lead to significantly improved binding free energies (e.g. protein–ligand systems) still lacks a clear answer.

In this manuscript, we probe the influence of the iodine MK radius on the obtained charges of iodinated molecules. Additionally, by using alchemical free energy

calculations to predict ΔG_{hyd} values, we also assess the influence of such radii in the hydration free energy of iodinated molecules when compared with experimental values.

2. Methods

2.1. *Molecules, charge models and RESP fitting procedure*

We selected all iodinated molecules with experimental ΔG_{hyd} values from the FreeSolv database.[26] A total of 12 compounds (iodoethane, 1-iodopropane, 2-iodopropane, 5-iodouracil, iodobenzene, iodomethane, 1-iodoheptane, 1-iodohexane, diiodomethane, 1-iodopentane, 1-iodobutane, and 2-iodophenol) were therefore used in this study. As described elsewhere,[16,17,24] the initial three-dimensional coordinates were obtained by performing geometry optimizations at the B3LYP/6-311G(d,p) level of theory. For the calculation of RESP[1] charges, the electrostatic potential (ESP) was generated at the HF/6-31G(d)[27–29] level of theory for all elements, except for iodine, for which we utilized the 6-311G(d)[30] basis set. For each molecule, the charges were fitted without and with the presence of an extra point of charge (EP), placed along the C–I covalent bond axis at a 2.15 Å distance, which corresponds to the Lennard-Jones (LJ) R_{min} parameter for iodine in GAFF, as suggested in reference 14. Succinctly, after the QM ESP is obtained, a massless particle is introduced in the multi-step RESP fitting step. The radii of the EPs are zero and therefore, they do not affect the number nor the distribution of the fitting points. Moreover, the penalty function employed during the RESP fitting procedure is also applied to this particle. An example of this procedure can be found in reference 31. For this fitting, the MK radius of iodine was varied between 1.00–4.00 Å using a step of 0.05 Å.

The fitting quality of the ESP generated by the obtained charges to the QM reference was evaluated by the relative root mean square (RRMS),[2] according to the following (eq 1)

$$RRMS = \left\{ \chi_{esp}^2 / \sum_i V_i^2 \right\}^{1/2} \tag{1}$$

with χ_{esp}^2 defined as (eq 2)

$$\chi_{esp}^2 = \sum_i (V_i - \hat{V}_i)^2 \tag{2}$$

and $\hat{V}_i$ being the calculated ESP.

2.2. *MD simulations and alchemical free energy calculations*

For three specific iodine MK radii (2.70 Å, 2.30 Å, and 1.98 Å, see Results and Discussion), the ΔG_{hyd} values were determined using alchemical free energy calculations employing a decoupling strategy based on the approach proposed by Mobley

and co-workers[32] and used by us in the assessment of halogen off-center point-charge models using explicit solvent simulations.[24] This involved 20 intermediate states in which the first 5 states corresponded to the turning-off of the electrostatic interactions, while the remaining 15 states slowly modified the Lennard-Jones terms. The simulations were performed using GROMACS version 2020.6 (CPU and GPU implementations),[33] the GAFF force field,[34] and the 2df type virtual site was used for the simulations with an off-center point charge.

Energy minimization, equilibration, and production runs were performed for each value of λ. In the minimization step, the steepest descent method was employed with a force threshold of 100.0 kJ mol^{-1} nm^{-1} and a maximum step size of 0.01 Å. Subsequently, three equilibration steps were performed using Langevin dynamics simulations. First, a 50 ps simulation was conducted in the canonical ensemble (NVT) at 298.15 K, followed by 50 ps in the isothermal-isobaric ensemble (NPT) using the Berendsen barostat at a pressure of 1 bar. Finally, an additional 5 ns run was carried out in NPT using the Parrinello-Rahman barostat. A time step of 2 fs was used for all equilibration steps.

After equilibration, three independent production runs of 5 ns were performed under the same conditions as the last equilibration step. The solutes were solvated with TIP3P water molecules in a cubic box employing three-dimensional periodic boundary conditions and the minimum image convention. The dimensions of the box were set to be at least twice the Lennard-Jones cutoff distance, following recommended practices,[35] and the maximum number of water molecules used per compound corresponded to the value reported in FreeSolv.[26] The van der Waals and electrostatic forces were truncated at a distance of 1.0 nm, long-range electrostatic interactions were treated using the fast smooth Particle-Mesh Ewald (PME) method, and bonds involving hydrogen atoms were constrained using the P-LINCS algorithm.

The reported ΔG_{hyd} values correspond to the average of the three replicates obtained using the Multistate Bennett Acceptance Ratio (MBAR)[36] method, implemented in the Alchemical Analysis python tool.[37] The standard error of the mean ($\pm$ 2×SEM, confidence of $\approx$ 95%) was used as an error estimate measure. Most compounds in this dataset lack reported experimental uncertainties, therefore, no statistical analysis could be performed in this scope.

To evaluate the accuracy of the ΔG_{hyd} values, the mean absolute error (MAE, eq. 3) and the root mean square deviation (RMSE, eq. 4) of the calculated against the experimental values were used.

$$\text{MAE} = n^{-1} \sum_{i=1}^{n} |\Delta G_{\text{hyd}}(\text{calc})_i - \Delta G_{\text{hyd}}(\text{exp})_i| \tag{3}$$

$$\text{RMSE} = \sqrt{n^{-1} \sum_{i=1}^{n} \left(\Delta G_{\text{hyd}}(\text{calc})_i - \Delta G_{\text{hyd}}(\text{exp})_i\right)^2} \tag{4}$$

3. Results and Discussion

3.1. *Influence of the iodine MK radii on the charges and quality of the RESP fitting*

As mentioned previously, the RESP charge model attributes partial atomic charges according to a fit of the calculated ESP to a reference potential obtained using a QM calculation. This is performed at a given number of grid points located on several layers around the molecule, using a molecular van der Waals surface generated with atomic radii, usually called Merz-Singh-Kollman (MK) radii. Typically, the lower layer is obtained by scaling the radii by a factor of 1.4. For iodine, there is no MK radii value available and therefore, we started by evaluating the quality of the fit of the ESP by obtaining the RRMS values for a range of radii values (1.00 Å to 4.00 Å, see Figure 2). In these calculations, we emulated the halogen anisotropy using an EP.[14] The same type of calculations were also conducted for models without EP (Figure 3). When using the standard RESP charges without the EP, the RRMS values typically decrease sharply till 2 Å, continuing to decrease slightly with the increase in the iodine MK radius as no minima are observed in the curves (Figures 3). The variation of iodine charge with the halogen radius using this model without EP shows an abrupt decrease, eventually reaching a plateau around 1.5 Å, though some differences can be observed among compounds, especially for diiodomethane. Nonetheless, it seems clear that at empirically-relevant radii values, the charges of iodine do not change significantly. Using an EP (Figure 2), the RRMS values also decrease and despite no minima being observed, it seems that a plateau is reached at radii values larger than 2.5 Å. For some compounds (e.g. 1-iodoheptane), this RRMS plateau is reached earlier. With this EP implementation, the iodine charges also decrease sharply with the increase of the iodine MK radius, however, the values are considerably more negative than those observed with the model without the EP. The variation of the EP charge is considerably lower than that observed for iodine, nonetheless, a slight increase in the charge is obtained with the decrease in the iodine MK radii values, reaching a plateau at around 1.5 Å. Notice that some peaks are observed in the RRMS and charge values at MK radius around 1.5 Å. This is probably due to the fact that, at this MK radii value, the first layer is placed very near the EP position (vertical yellow line in Figure 2). Indeed, since we used the default MK scheme which adds three layers constructed with scaling factors of 1.4, 1.6, 1.8, and 2.0 Å, an MK iodine radius of 1.5 Åwould put the first layer at 2.1 Å, which overlaps with the EP (2.15 Å).

Both the EP and no EP results indicate that there is no evident "ideal" iodine MK radius based on the quality of the fit (RRMS values), and in fact, the values decrease with increasing radius. However, as mentioned previously, the RRMS decreases considerably until an iodine radius of 2 Åis reached, and thus, the assignment of a lower value might not be recommended.
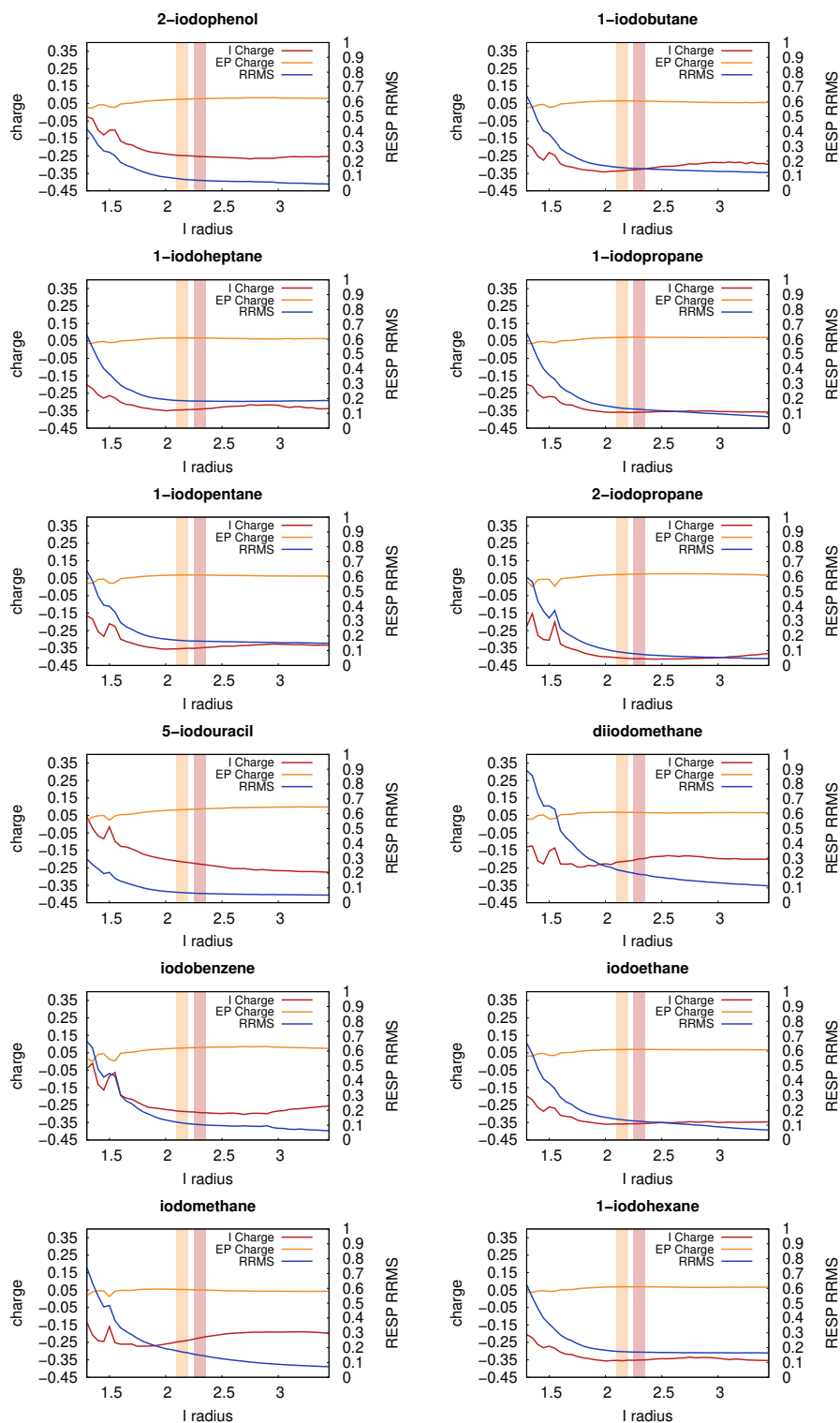
Fig. 2. Variation of the ESP RRMS values (providing the quality of the fit) along with the EP and iodine charges (assigned during the RESP fitting) as a function of the iodine MK radius. The vertical orange line corresponds to the iodine radius of 2.3 Å, commonly used by our group, and the vertical yellow line represents the distance at which the EP is placed (2.15 Å).
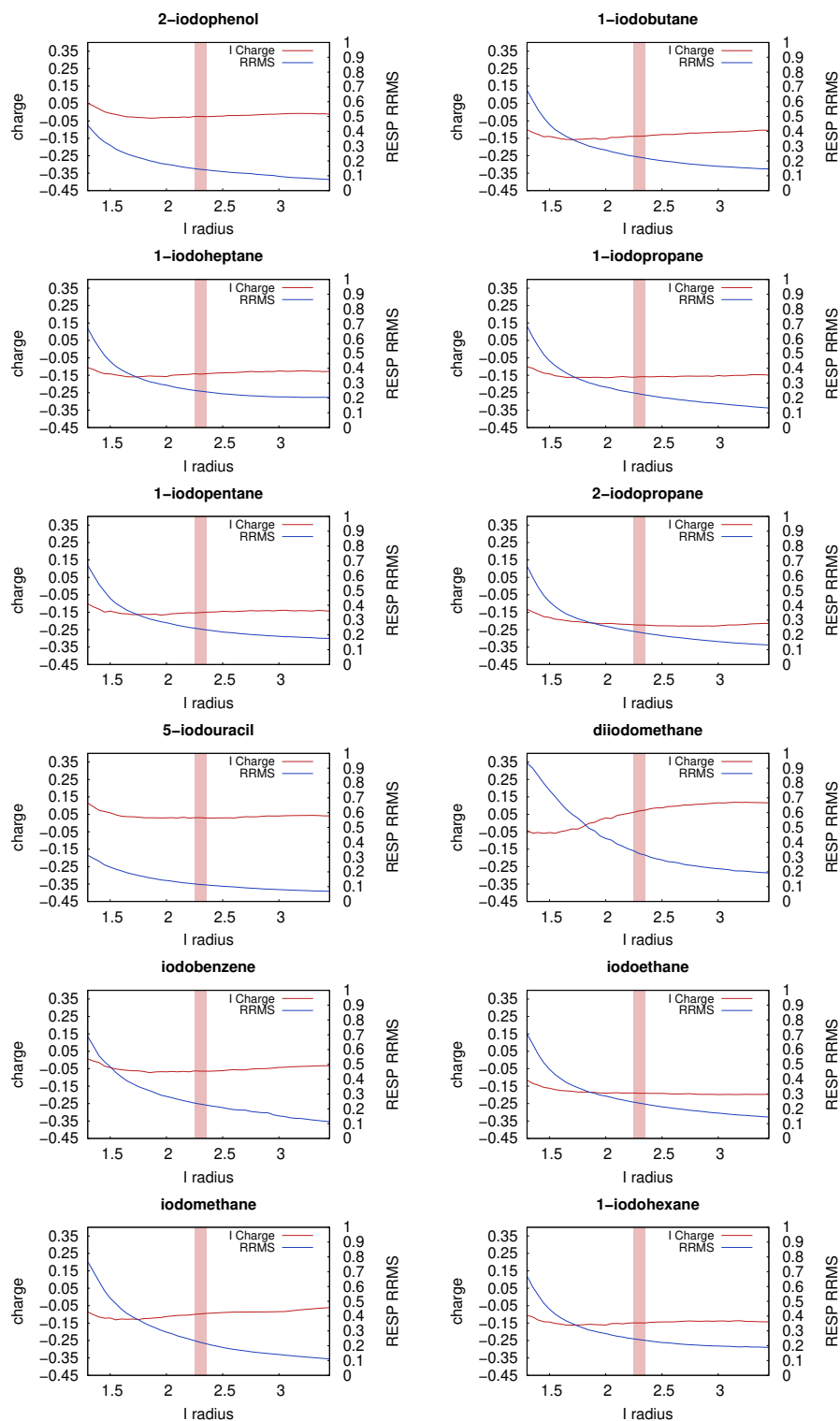
Fig. 3. Variation of the ESP RRMS (providing the quality of the fit) along with the iodine charge (assigned during the RESP fitting without an EP) as a function of the iodine MK radius. The vertical orange line corresponds to the iodine radius of 2.3 Å, commonly used by our group.

3.2. *Performance of different MK iodine radii in the determination of ΔG_{hyd}*

Since no hints could be inferred from the previous section regarding a proper iodine radius, we performed alchemical free energy calculations to predict the ΔG_{hyd} values of our set of iodinated molecules. Notice that the calculation of ΔG_{hyd} is highly sensitive to the charges used in the force field[38] and therefore, these values are commonly used for force field validation. For practical reasons, only three MK radii values were utilized: 1.98 Å which is often taken as a reference value for the iodine van der Waals radius,[39] 2.30 Å that has been used by us in previous studies,[15–17, 24] and 2.70 Å which was previously employed in the assessment of the effect of EPs on the partial charges of halogenated molecules.[23] The MAE and RMSE values obtained for each iodine MK radii and charge model tested (with and without EP) are presented in Table 1. When no extra point with a partial atomic charge is used,

Table 1. MAE and RMSE (kcal mol^{-1}) values obtained using different MK iodine radii, with and without EP

	no EP		EP	
MK radius (Å)	MAE	RMSE	MAE	RMSE
1.98	0.85	1.09	0.81	0.95
2.30[24]	0.81	1.09	0.87	0.97
2.70	0.76	1.06	0.79	0.89

the MAE values decrease with increasing MK radius while the RMSE also decreases from 1.98 and 2.30 Å to 2.70 Å. This tendency is not observed in the presence of an EP. Despite the clear agreement of the lowest MAE and RMSE values also being obtained with a MK radius of 2.70 Å (0.79 and 0.89 kcal mol^{-1}, respectively), the radius with the worst performance is now the 2.30 Å. Although the differences are not substantial in some cases, we can argue that the best performance was obtained using the iodine MK radius of 2.70 Åfor both the EP and no EP models. This radius also shortened the difference in the performance of EP *versus* the no EP model observed in our earlier study using 2.30 Å.[24]

We analyzed further the calculated ΔG_{hyd} values by looking at the maximum of the electrostatic potential at iodine ($V_{S,max}$) for each compound, which is a measure of the σ–hole strength and is often used as an XB strength predictor.[3] The values are collected in Tables 2 and 3 for charges obtained without and with EP, respectively. Curiously, for the compounds with the highest $V_{S,max}$, for which the XBs are expected to be important, some trends were verified. Indeed, using an EP, the prediction of the ΔG_{hyd} of 5-iodouracil ($V_{S,max} = 24.36$ kcal mol^{-1}) and 2-iodophenol ($V_{S,max} = 14.73$ kcal mol^{-1}) improved considerably (lower deviation between experimental and calculated ΔG_{hyd}) with the increase of the iodine ra-

Table 2. Experimental ($\Delta G_{\text{hyd}}(\text{exp})$) and calculated ($\Delta G_{\text{hyd}}(\text{calc})$) hydration free energies (kcal mol^{-1}) obtained using different iodine MK radius and standard RESP charges (no EP). The $V_{S,max}$ corresponds to the maxima of the electrostatic potential (ESP) at the iodine for each compound (kcal mol^{-1}), computed at the B3LYP/6-311G(d,p) level.

compound	$\Delta G_{\text{hyd}}(\text{exp})$[26]	$\mathbf{V}_{S,max}$	$\Delta G_{\text{hyd}}(\text{calc})$		
			1.98 Å	**2.30 Å**[24]	**2.70 Å**
iodoethane	-0.74	10.17	-0.01 ± 0.02	-0.04 ± 0.01	0.01 ± 0.01
1-iodopropane	-0.53	9.93	-0.11 ± 0.04	-0.13 ± 0.03	-0.10 ± 0.05
2-iodopropane	-0.46	7.33	-0.04 ± 0.02	-0.07 ± 0.04	-0.01 ± 0.02
5-iodouracil	-18.72	24.36	-16.64 ± 0.02	-16.37 ± 0.05	-16.24 ± 0.05
iodobenzene	-1.74	16.59	-0.92 ± 0.03	-1.01 ± 0.03	-1.09 ± 0.01
iodomethane	-0.89	12.68	-0.12 ± 0.04	-0.23 ± 0.01	-0.20 ± 0.01
1-iodoheptane	0.27	9.29	0.42 ± 0.02	0.39 ± 0.04	0.41 ± 0.04
1-iodohexane	0.08	9.36	0.30 ± 0.02	0.29 ± 0.04	0.35 ± 0.07
diiodomethane	-2.49	21.68	-0.86 ± 0.02	-1.54 ± 0.06	-2.11 ± 0.02
1-iodopentane	-0.14	9.44	0.28 ± 0.04	0.27 ± 0.03	0.27 ± 0.04
1-iodobutane	-0.25	9.63	0.10 ± 0.01	0.08 ± 0.03	0.02 ± 0.00
2-iodophenol	-6.20	14.73	-3.99 ± 0.07	-3.75 ± 0.20	-3.94 ± 0.09

dius (5-iodouracil: 1.42 *vs* 0.71 *vs* -0.02 kcal mol^{-1}; 2-iodophenol: 1.83 vs 1.66 vs 1.27 kcal mol^{-1}), as presented in Table 3. If the halogen anisotropy is not included *via* an EP (Table 2), the prediction of the ΔG_{hyd} is worse for these compounds, with deviations around 2 kcal mol^{-1}. Nonetheless, the usage of a 2.70 Å radius yields the best results even without the EP. We should note that the opposite trend was verified for diiodomethane ($V_{S,max} = 21.68$ kcal mol^{-1}) and iodobenzene ($V_{S,max} = 16.59$ kcal mol^{-1}), for which the prediction of the ΔG_{hyd} got worse with the increase of the iodine MK radius using the EP model (diiodomethane: 0.02 *vs* 0.04 *vs* 0.21; iodobenzene: -0.19 *vs* -0.73 *vs* -1.17 kcal mol^{-1}). The same tendency was observed without the EP usage (diiodomethane: 0.38 *vs* 0.95 *vs* 1.63 kcal mol^{-1}; iodobenzene: 0.65 *vs* 0.73 *vs* 0.82 kcal mol^{-1}). These trends can also be observed in Figure 4, which shows a comparison between the experimental and calculated ΔG_{hyd} values using the different iodine MK radius used. Without the use of an EP, there is a tendency to overestimate the ΔG_{hyd} values as their calculated values are systematically more positive than the experimental ones. This deviation seems to increase as the experimental ΔG_{hyd} values become more negative showing that, without emulating the anisotropy, the predictions become harder for the more hydrophilic compounds, with the MK radius of 2.70 Å yielding the best results. A different tendency is obtained when we consider the iodine anisotropy (EP). Here, the calculated ΔG_{hyd} have a tendency to be underestimated (too negative) for the most hydrophobic compounds, indicating that the extra point might introduce an

Table 3. Experimental (ΔG_{hyd}(exp)) and calculated (ΔG_{hyd}(calc)) hydration free energies (kcal mol^{-1}) obtained using different iodine MK radius using the EP model.[14] The $V_{S,max}$ corresponds to the maxima of the electrostatic potential (ESP) at the iodine for each compound (kcal mol^{-1}), computed at the B3LYP/6-311G(d,p) level.

compound	ΔG_{hyd}(exp)[26]	$V_{S,max}$	ΔG_{hyd}(calc)		
			1.98 Å	2.30 Å[24]	2.70 Å
iodoethane	-0.74	10.17	-1.25 ± 0.05	-1.44 ± 0.01	-1.34 ± 0.03
1-iodopropane	-0.53	9.93	-1.41 ± 0.04	-1.59 ± 0.03	-1.55 ± 0.03
2-iodopropane	-0.46	7.33	-1.44 ± 0.07	-1.83 ± 0.06	-1.90 ± 0.03
5-iodouracil	-18.72	24.36	-17.30 ± 0.05	-18.02 ± 0.07	-18.74 ± 0.04
iodobenzene	-1.74	16.59	-1.93 ± 0.02	-2.47 ± 0.07	-2.91 ± 0.01
iodomethane	-0.89	12.68	-0.71 ± 0.05	-0.70 ± 0.01	-0.63 ± 0.01
1-iodoheptane	0.27	9.29	-0.79 ± 0.01	-0.94 ± 0.07	-0.79 ± 0.01
1-iodohexane	0.08	9.36	-0.92 ± 0.01	-0.98 ± 0.03	-0.87 ± 0.04
diiodomethane	-2.49	21.68	-2.47 ± 0.03	-2.45 ± 0.00	-2.28 ± 0.03
1-iodopentane	-0.14	9.44	-1.03 ± 0.03	-1.04 ± 0.06	-0.90 ± 0.04
1-iodobutane	-0.25	9.63	-1.00 ± 0.03	-1.07 ± 0.04	-0.92 ± 0.03
2-iodophenol	-6.20	14.73	-4.37 ± 0.06	-4.54 ± 0.12	-4.93 ± 0.05

overestimated amphoteric character to these specific compounds regardless of the radii used.

Overall, despite the usage of an MK radius of 2.30 Å to fit RESP charges (both with and without EP) does not lead to a dramatic error on the calculated ΔG_{hyd} values, our results point out that a value of 2.70 Å leads to a better agreement with the experimental values. Nonetheless, and given the different nature of the compounds and the reduced size of this library, this question is not completely closed and this work might also fuel the experimentalists to provide data on additional iodinated compounds to improve our force field parametrizations.

4. Conclusions

Traditional force field methods rely on point charges to describe the electrostatic interactions. In this scope, the RESP procedure is one of the most used methods. This model requires van der Waals radii (or MK radii) in addition to a reference electrostatic potential to build layers of grid points around the molecule. Such radius for iodine is unknown and in the literature, to the best of our knowledge, two values have been used, 2.30 Å[15–17] and 2.70Å.[23] Herein, we studied the effect of changing the MK radius of iodine during the RESP fitting procedure on the quality of the fit and charges on a set of 12 iodinated molecules taken from the FreeSolv database.[26] By varying the iodine radius, the RRMS values obtained with and without an extra point (EP), which emulates the halogen σ–hole, kept decreasing with increasing
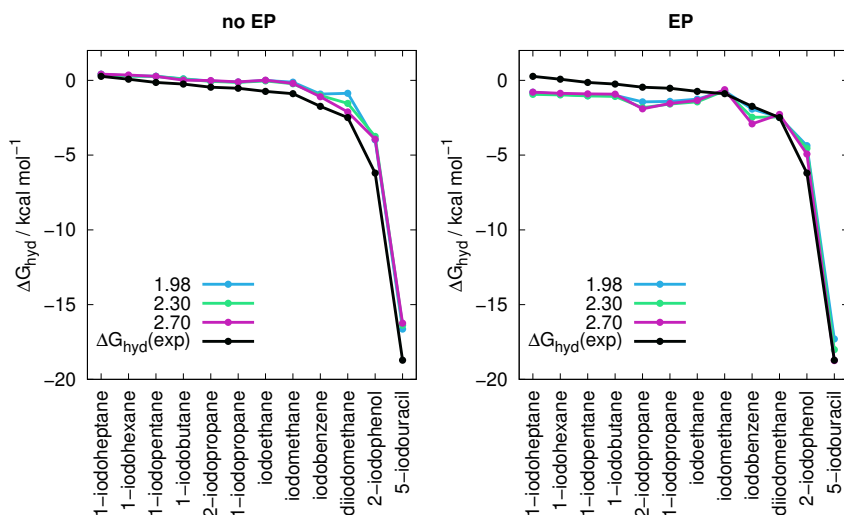
Fig. 4. Experimental (black) and calculated ΔG_{hyd} using iodine MK radius of 1.98 Å(blue), 2.30 Å(green) and 2.70 Å(purple), using standard RESP charges (no EP) and the EP implementation, for each iodinated compound in the study. The compounds are sorted by their experimental ΔG_{hyd} values.

radii for most compounds, which makes this property (quality of the fit) impractical for radii optimization. Nevertheless, the RRMS values exhibited a substantial decrease until the iodine radius reached approximately 2 Å. Therefore, assigning a lower radius value is not advisable. Since ΔG_{hyd} values are extremely sensitive to the atomic partial charges used in the force field, we performed alchemical free energy calculations to evaluate the influence of such radii in the ΔG_{hyd} values for three iodine MK radius: 1.98 Å, 2.30 Å, and 2.70 Å. Overall, the MAE and RMSE values obtained indicate that the usage of different iodine MK radii does not lead to a remarkable difference in the calculated values, however, using a value of 2.70Å systematically led to lower MAE and RMSE values when comparing experimental and calculated ΔG_{hyd} values. When no anisotropy is emulated (no EP), the agreement between calculated and experimental values is worse as the experimental ΔG_{hyd} values become more negative. When an EP is added, the performance is better for compounds with a larger $V_{S,max}$. With this work, we aimed to contribute to a further refinement of the halogen bond description using force field methods.

Conflict of Interest

One of the corresponding authors (M.M.) declares that, as an associate editor of the present journal, there is a conflict of interest regarding this manuscript. However, M.M. confirms that he was not involved in the peer review procedure of this

manuscript, and therefore, he did not influence the editorial decision-making process. The conflict of interest was disclosed to the editorial team, and appropriate steps were taken to ensure that the peer review and decision-making process for this manuscript were handled impartially and transparently.

Funding Information

References

1. Wang, J.; Wang, W.; Kollman, P. A.; Case, D. A. Automatic atom type and bond type perception in molecular mechanical calculations. *J. Mol. Graph. Model.* **2006**, *25*, 247–260.
2. Bayly, C. I.; Cieplak, P.; Cornell, W.; Kollman, P. A. A well-behaved electrostatic potential based method using charge restraints for deriving atomic charges: the RESP model. *J. Phys. Chem.* **1993**, *97*, 10269–10280.
3. Clark, T.; Hennemann, M.; Murray, J. S.; Politzer, P. Halogen bonding: the σ-hole. *J.Mol. Model.* **2007**, *13*, 291–296.
4. Desiraju, G. R.; Ho, P. S.; Kloo, L.; Legon, A. C.; Marquardt, R.; Metrangolo, P.; Politzer, P.; Resnati, G.; Rissanen, K. Definition of the halogen bond (IUPAC Recommendations 2013). *Pure Appl. Chem.* **2013**, *85*, 1711–1713.
5. Costa, P. J. The halogen bond: nature and applications. *Phys. Sci. Rev.* **2017**, *2*, 20170136.
6. Auffinger, P.; Hays, F. A.; Westhof, E.; Ho, P. S. Halogen bonds in biological molecules. *Proc. Natl. Acad. Sci.* **2004**, *101*, 16789–16794.
7. Wilcken, R.; Zimmermann, M. O.; Lange, A.; Joerger, A. C.; Boeckler, F. M. Principles and applications of halogen bonding in medicinal chemistry and chemical biology. *J. Med. Chem.* **2013**, *56*, 1363–1388.
8. Costa, P. J.; Nunes, R.; Vila-Viçosa, D. Halogen bonding in halocarbon-protein complexes and computational tools for rational drug design. *Expert Opin. Drug Discov.* **2019**, *14*, 805–820.
9. Frontera, A.; Bauzá, A. Halogen bonds in protein nucleic acid recognition. *J. Chem. Theory Comput.* **2020**, *16*, 4744–4752.
10. Nunes, R. S.; Vila-Viçosa, D.; Costa, P. J. Halogen bonding: an underestimated player in membrane–ligand interactions. *J. Am. Chem. Soc.* **2021**, *143*, 4253–4267.
11. Sutar, R. L.; Engelage, E.; Stoll, R.; Huber, S. M. Bidentate chiral bis (imidazolium)-based halogen-bond donors: synthesis and applications in enantioselective recognition and catalysis. *Angew. Chem. Int. Ed.* **2020**, *59*, 6806–6810.

12. Yang, H.; Wong, M. W. Application of halogen bonding to organocatalysis: A theoretical perspective. *Molecules* **2020**, *25*, 1045.
13. Vanderkooy, A.; Taylor, M. S. Exploring the construction of multicompartmental micelles by halogen bonding of complementary macromolecules. *Faraday Discuss.* **2017**, *203*, 285–299.
14. Ibrahim, M. A. Molecular mechanical study of halogen bonding in drug discovery. *J. Compt. Chem.* **2011**, *32*, 2564–2574.
15. Nunes, R.; Vila-Vicosa, D.; Machuqueiro, M.; Costa, P. J. Biomolecular simulations of halogen bonds with a GROMOS force field. *J. Chem. Theory Comput..* **2018**, *14*, 5383–5392.
16. Fortuna, A.; Costa, P. J. Optimized Halogen Atomic Radii for PBSA Calculations Using Off-Center Point Charges. *J. Chem. Inf. Model.* **2021**, *61*, 3361–3375.
17. Nunes, R.; Vila-Viçosa, D.; Costa, P. J. Tackling Halogenated Species with PBSA: Effect of Emulating the σ-hole. *J. Chem. Theory Comput.* **2019**, *15*, 4241–4251.
18. Ibrahim, M. A. A. Molecular mechanical perspective on halogen bonding. *J. Mol. Model.* **2012**, *18*, 4625–4638.
19. Singh, U. C.; Kollman, P. A. An approach to computing electrostatic charges for molecules. *J. Comput. Chem* **1984**, *5*, 129–145.
20. Sun, Y.; He, X.; Hou, T.; Cai, L.; Man, V. H.; Wang, J. Development and test of highly accurate endpoint free energy methods. 1: Evaluation of ABCG2 charge model on solvation free energy prediction and optimization of atom radii suitable for more accurate solvation free energy prediction by the PBSA method. *J. Compt. Chem.* **2023**, *44*, 1334–1346.
21. Mecklenfeld, A.; Raabe, G. Comparison of RESP and IPolQ-mod partial charges for solvation free energy calculations of various solute/solvent pairs. *J. Chem. Theory Comput.* **2017**, *13*, 6266–6274.
22. Wang, J.; Hou, T. Application of molecular dynamics simulations in molecular property prediction. 1. density and heat of vaporization. *J. Chem. Theory Comput.* **2011**, *7*, 2151–2165.
23. Leskourová, A.; Kolář, M. H. The effect of off-center σ–hole on the atom-centered partial charges in halogenated molecules. *J. Comput. Chem.* **2022**, *43*, 864–869.
24. Fortuna, A.; Costa, P. J. Assessment of Halogen Off-Center Point-Charge Models Using Explicit Solvent Simulations. *ChemRxiv* **2023**, *10.26434/chemrxiv-2023-sgbfb*.
25. Costa, P. J.; Nunes, R. In *Frontiers in Computational Chemistry: Volume 4*; Ul-Haq, Z., Wilson, A. K., Eds.; Bentham Science Publishers: Sharjah, UAE, 2018; Chapter 4, pp 144–183.
26. Mobley, D. L. FreeSolv, version 0.51. 2013; `http://www.escholarship.org/uc/item/6sd403pz` (accessed october 2023).
27. Hariharan, P. C.; Pople, J. A. The influence of polarization functions on molecular orbital hydrogenation energies. *Theor. Chim. Acta* **1973**, *28*, 213–222.
28. Francl, M. M.; Pietro, W. J.; Hehre, W. J.; Binkley, J. S.; Gordon, M. S.; DeFrees, D. J.; Pople, J. A. Self-consistent molecular orbital methods. XXIII. A polarization-type basis set for second-row elements. *J. Chem. Phys.* **1982**, *77*, 3654–3665.
29. Rassolov, V. A.; Ratner, M. A.; Pople, J. A.; Redfern, P. C.; Curtiss, L. A. 6-31G* basis set for third-row atoms. *J. Comput. Chem.* **2001**, *22*, 976–984.
30. Glukhovtsev, M. N.; Pross, A.; McGrath, M. P.; Radom, L. Extension of Gaussian-2 (G2) theory to bromine-and iodine-containing molecules: Use of effective core potentials. *J. Chem. Phys.* **1995**, *103*, 1878–1885.
31. Costa, P. J. *Transmembrane Anion Transport Mediated by Halogen Bonds: Using Off-*

Center Charges; Springer, 2021; pp 273–284.

32. Duarte Ramos Matos, G.; Kyu, D. Y.; Loeffler, H. H.; Chodera, J. D.; Shirts, M. R.; Mobley, D. L. Approaches for calculating solvation free energies and enthalpies demonstrated with an update of the FreeSolv database. *J. Chem. Eng. Data* **2017**, *62*, 1559–1569.

33. Abraham, M. J.; Murtola, T.; Schulz, R.; Páll, S.; Smith, J. C.; Hess, B.; Lindahl, E. GROMACS: High performance molecular simulations through multi-level parallelism from laptops to supercomputers. *SoftwareX* **2015**, *1*, 19–25.

34. Wang, J.; Wolf, R. M.; Caldwell, J. W.; Kollman, P. A.; Case, D. A. Development and testing of a general amber force field. *J. Comp. Chem.* **2004**, *25*, 1157–1174.

35. Gapsys, V.; de Groot, B. L. On the importance of statistics in molecular simulations for thermodynamics, kinetics and simulation box size. *Elife* **2020**, *9*, e57589.

36. Shirts, M. R.; Chodera, J. D. Statistically optimal analysis of samples from multiple equilibrium states. *J. Chem. Phys.* **2008**, *129*, 124105.

37. Klimovich, P. V.; Shirts, M. R.; Mobley, D. L. Guidelines for the analysis of free energy calculations. *J. Comput. Aided Mol. Des.* **2015**, *29*, 397–411.

38. Jämbeck, J. P.; Mocci, F.; Lyubartsev, A. P.; Laaksonen, A. Partial atomic charges and their impact on the free energy of solvation. *J. Comp. Chem.* **2013**, *34*, 187–197.

39. Bondi, A. v. van der Waals volumes and radii. *J. Phys. Chem. Lett.,* **1964**, *68*, 441–451.